



Antiviral activity of traditional medicinal plants from Ayurveda against SARS-CoV-2 infection

Vimal K. Maurya[#], Swatantra Kumar, Madan L. B. Bhatt and Shailendra K. Saxena[#]

Department of Centre for Advanced Research (CFAR), Faculty of Medicine, King George's Medical University (KGMU), Lucknow, India

Communicated by Ramaswamy H. Sarma

ABSTRACT

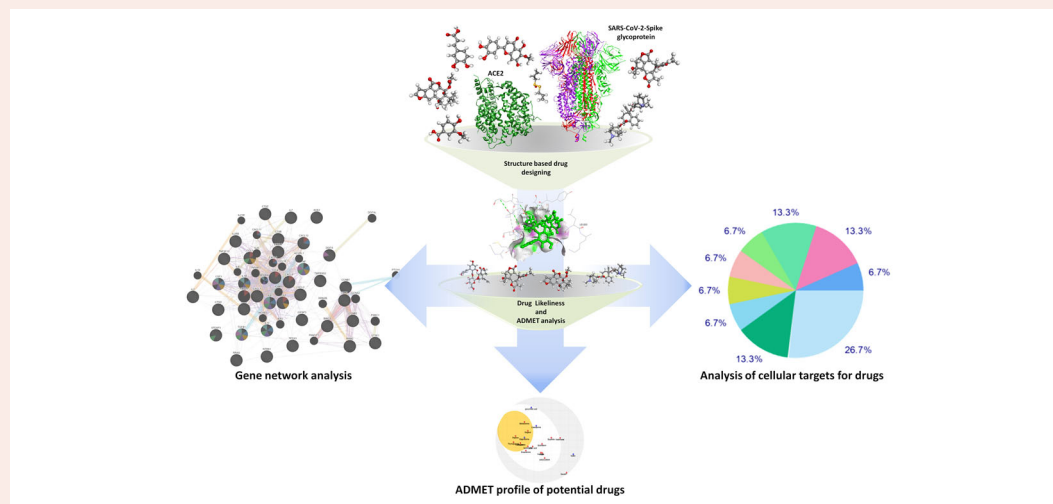
SARS-CoV-2 is the etiological agent of COVID-19 and responsible for more than 6 million cases globally, for which no vaccine or antiviral is available. Therefore, this study was planned to investigate the antiviral role of the active constituents against spike glycoprotein of SARS-CoV-2 as well as its host ACE2 receptor. Structure-based drug design approach has been used to elucidate the antiviral activity of active constituents present in traditional medicinal plants from Ayurveda. Further, parameters like drug-likeness, pharmacokinetics, and toxicity were determined to ensure the safety and efficacy of active constituents. Gene network analysis was performed to investigate the pathways altered during COVID-19. The prediction of drug-target interactions was performed to discover novel targets for active constituents. The results suggested that amarogentin, eufoliatorin, α -amyrin, caesalpinins, kutkin, β -sitosterol, and belladonnine are the top-ranked molecules have the highest affinity towards both the spike glycoprotein and ACE2. Most active constituents have passed the criteria of drug-likeness and demonstrated good pharmacokinetic profile with minimum predicted toxicity level. Gene network analysis confirmed that G-protein coupled receptor, protein kinase B signaling, protein secretion, peptidyl-serine phosphorylation, nuclear transport, apoptotic pathway, tumor necrosis factor, regulation of angiotensin level, positive regulation of ion transport, and membrane protein proteolysis were altered during COVID-19. The target prediction analysis revealed that most active constituents target the same pathways which are found to be altered during COVID-19. Collectively, our data encourages the use of active constituents as a potential therapy for COVID-19. However, further studies are ongoing to confirm its efficacy against disease.

ARTICLE HISTORY

Received 15 June 2020
Accepted 30 September 2020

KEYWORDS

SARS-CoV-2; COVID-19; structure-based drug design; attachment inhibitor; gene network analysis; target prediction; pharmacokinetics; Ayurveda



Abbreviations: ACE2: (Angiotensin-converting enzyme 2); BIRC5: (Baculoviral IAP Repeat Containing 5); CCL2: (Chemokine (C-C motif) ligand 2); CCL3: (Chemokine (C-C motif) ligand 3); CCL3: (Chemokine (C-C motif) ligand 3); CCL4: (C-C Motif Chemokine Ligand 4); CCNB1: (Cyclin B1); CCNB2: (Cyclin B2); CDK1: (Cyclin-dependent kinase 1); COVID-19: (Coronavirus disease); CSF3: (Colony Stimulating Factor 3); CTSB: (Cathepsin B); CTSD: (Cathepsin D); CTSL: (Cathepsin L); CTSZ: (Cathepsin Z); CXCL1: (Chemokine (C-X-C motif) ligand 1); CXCL10: (C-X-C motif chemokine 10); CXCL2: (Chemokine (C-X-C

CONTACT Shailendra K. Saxena shailen@kgmcindia.edu Department of Centre for Advanced Research, Faculty of Medicine, King George's Medical University (KGMU), Lucknow, 226003, India

[#]These authors contributed equally to this work.

Supplemental data for this article can be accessed online at <https://doi.org/10.1080/07391102.2020.1832577>

© 2020 Informa UK Limited, trading as Taylor & Francis Group

motif ligand 2); CXCL6: (Chemokine (C-X-C motif) ligand 6); CXCL8: (Interleukin 8); DDIT4: (DNA-damage-inducible transcript 4); GTSE1: (G2 and S-Phase Expressed 1); IGFBP3: (Insulin Like Growth Factor Binding Protein 3); IL-10: (Interleukin 10); IL1B: (Interleukin 1 beta); IL2: (Interleukin 2); IL2RB: (Interleukin-2 receptor subunit beta); IL-6: (Interleukin 6); IL7: (Interleukin 7); MERS-CoV: (Middle East respiratory syndrome coronavirus); NTRK1: (Neurotrophic Receptor Tyrosine Kinase 1); RRM2: (Ribonucleotide Reductase Regulatory Subunit M2); SARS-CoV: (Severe acute respiratory syndrome coronavirus); SARS-CoV-2: (Severe acute respiratory syndrome coronavirus 2); STEAP3: (Six-Transmembrane Epithelial Antigen of Prostate 3); TGFB1: (Transforming growth factor beta 1); TMPRSS2: (Transmembrane protease serine 2); TNF: (Tumour necrosis factor); TNFSF10: (Tumor Necrosis Factor (Ligand) Superfamily, Member 10); TP53I3: (Tumor Protein P53 Inducible Protein 3)

Introduction

Since December 2019, there has been a significant threat to world health from a new coronavirus pneumonia pandemic called Coronavirus disease (COVID-19) (Chen et al., 2020). The infection is caused by a new coronavirus strain named severe acute respiratory syndrome coronavirus-2 (SARS-CoV-2), an enveloped RNA virus of the genus *Betacoronavirus* described as the 7th member of the *Coronaviridae* family reported in humans (Andersen et al., 2020). This new coronavirus was firstly confirmed in Wuhan City, Hubei, China whereas the first human-to-human transmission was reported in Guangdong, China (Singhal, 2020). The rate of SARS-CoV-2 transmission has been shown to be higher as compared to the previous coronavirus outbreaks. As of 2nd June 2020, SARS-CoV-2 almost reaches every country in the world with more than 6 million confirmed cases and 0.37 million deaths around the globe (<https://www.who.int/emergencies/diseases/novel-coronavirus-2019>). Patients reported with COVID-19 presents wide range of clinical symptoms including headache, fever, shortness of breath, coughing, vomiting, chills, dyspnea, sore throat, myalgia, diarrhea, malaise and neurological complications like Guillain-Barre syndrome, encephalopathy, necrotising hemorrhagic encephalopathy, epileptic seizures, encephalitis, stroke, and rhabdomyolysis. The severe infection associated with acute respiratory distress syndrome (ARDS), pneumonia, multi-organ failures and even death (Guan et al., 2020).

After the analysis of viral sequence and evolutionary trend, bats were believed to be the natural reservoir of the SARS-CoV-2 and may have been shifted to humans as transitional hosts. Sequence alignment of spike glycoprotein of SARS-CoV-2 with SARS-CoV demonstrated higher sequence similarity than that of MERS-CoV with the least structural divergence (Kumar et al., 2020). The SARS-CoV-2 genome (30 kb in size) encodes four structural proteins: spike glycoprotein (S), envelope protein (E), matrix glycoprotein (M) and nucleocapsid protein (N), non-structural polyproteins, open reading frame (ORF) 1a/b and five accessory proteins (ORF9, ORF8, ORF7, ORF6, and ORF3a). These proteins are highly essential for assembly and infection of SARS-CoV-2 (Guo et al., 2020; Kumar et al., 2020). The spike glycoprotein present in SARS-CoV-2 serves as a viral antigen and is responsible for binding the host-receptor, internalizing the virus, triggering strong immune response (humoral and cell-mediated) during infection. Binding of SARS-CoV-2 with angiotensin-converting enzyme 2 (ACE2) facilitates virus entry into

the host cells (Belouzard et al., 2012). Therefore, this property of spike glycoprotein can be targeted for the development of potential attachment inhibitors against SARS-CoV-2 infection.

Considering the widespread nature of infection, no licensed antiviral agent is available for the treatment of SARS-CoV-2 infection. Medicinal drugs identified from the plants exhibited promising sources of potential and cost-effective therapy and may accelerate the drug discovery process during humanitarian emergencies. Plants such as *Allium cepa*, *Allium sativum*, *Alstonia scholaris*, *Artemisia vulgaris*, *Atropa belladonna*, *Caesalpinia crista*, *Glycyrrhiza glabra*, *Nigella sativa*, *Picrorhiza kurroa*, *Piper nigrum*, *Swertia chirata*, *Tinospora cordifolia* and *Zingiber officinale* are listed in AYUSH (Ayurveda, Unani, Siddha, and Homeopathy) system of medicine and traditionally used to treat flu-like symptoms (headache, fever, sore throat, cough, and runny nose). Therefore, we have planned to investigate the active constituents present in these medicinal plants for possible antiviral activity against spike glycoprotein of SARS-CoV-2 as well as its host ACE2 receptor using structure-based drug design method. The name, 3D structures and pharmacological functions of selected active constituents were presented in Table 1.

Material and methods

Ligand retrieval

The 3D (3 dimensional) structures of amarogentin (CID:115149), sawertiamarine (CID:442435), α -amyrin (CID:5471661), β -sitosterol (CID:222284), caesalpinins (CID:11419457), kutkin (CID:131750183), vanillic acid (CID:8468), 6-gingerol (CID:442793), glycyrrhetic acid (CID:9897771), piperine (CID: 638024), magnoflorine (CID:73337), alliin (CID:87310), allicin (CID:65036), n-acetylcysteine (CID:12035), thymoquinone (CID:10281), atropine (CID:174174), hyoscyamine (CID:154417), scopolamine (CID:3000322), belladonnine (CID:442995), eufolatorin (CID:21677945), eupafolin (CID:5317284), and caffeic acid (CID:689043) were retrieved from the NCBI PubChem compound database (<https://pubchem.ncbi.nlm.nih.gov/>) in SDF format and optimized with the help of Biovia Discovery Studio (<https://www.3dsbiovia.com/products/collaborative-science/biovia-discoverystudio/visualization>). The canonical SMILES of selected active constituents were presented in (supplementary Table 1).

Protein retrieval

The 3D crystal structure of spike glycoprotein (PDB ID: 6VXX) and its receptor ACE2 (PDB ID: 1R42) were obtained from the Research Collaboratory for Structural Bioinformatics (RCSB) Protein Data Bank (<https://www.rcsb.org/>) (Towler et al., 2004; Walls et al., 2020). The protein preparation was performed using the biovia discovery studio tool. All the inhibitors and cofactors that are co-crystallized with protein were selected, removed and hydrogens were added to the proteins.

Structure-based drug design using molecular docking

Structure-based drug design approach was applied to discover novel attachment inhibitors from traditional medicinal plants. Docking of selected active constituents with spike glycoprotein and ACE2 was performed with the help of Molegro Virtual Docker (MVD-3.0.0). Cavity or ligand binding site of proteins were determined. MVD showed higher docking accuracy when benchmarked against other available docking programs (MD: 87%, Glide: 82%, Surflex: 75%, FlexX:58%) and has been shown to be successful in several recent studies, but also for reasons of cost and user friendliness (Thomsen & Christensen, 2006). Commonly, 5 cavities were detected in the protein and cavity having maximum volume and surface area was used for the docking of active constituents. Nafamostat (Li & De Clercq, 2020) (inhibitor of spike glycoprotein) and captopril (inhibitor of ACE2) have been taken as a control for selected active constituents. For spike glycoprotein, docking scores of selected active constituents were compared with nafamostat; for angiotensin-converting enzyme-2, docking scores of selected active constituents were compared with captopril. The selected active constituents showing higher docking scores than nafamostat and captopril were considered to be the potent inhibitors of the spike glycoprotein and angiotensin-converting enzyme-2 respectively (Maurya et al., 2020).

Absorption, distribution, metabolism, and excretion (ADME) prediction

The drug-likeness and pharmacokinetics (ADME) properties of selected active constituents were examined via swissADME server (<http://www.swissadme.ch>) (Daina et al., 2017). The parameters such as gastro-intestinal absorption (GIA), P-gp substrate, blood-brain barrier (BBB) permeability, CYP2C9 inhibitor, CYP1A2 inhibitor, CYP2D6 inhibitor, CYP2C19 inhibitor, CYP3A4 inhibitor properties of selected active constituents were calculated.

Toxicity prediction

ProTox-II server (http://tox.charite.de/protox_II/) was used for the toxicity prediction of selected active constituents (Banerjee et al., 2018). ProTox-II offers the prediction of various toxicity endpoints such as adverse outcomes (Tox21) pathways, and acute toxicity, hepatotoxicity, carcinogenicity,

cytotoxicity, mutagenicity, immunotoxicity of selected active constituents.

Gene network and pathway analysis

To elucidate the gene network and pathway analysis, articles available in PubMed, MEDLINE and Cochrane library were searched using keywords 'SARS-CoV-2 and gene expression' or 'COVID-19 and gene expression' or '2019-nCoV and gene expression' and articles published between 1 Jan 2020 to 15 May 2020 were considered for this study. Significantly altered genes during COVID-19 were identified and biological networks of genes and associated pathways were analyzed using GeneMANIA web server (<http://genemania.org>) (Franz et al., 2018).

Target prediction

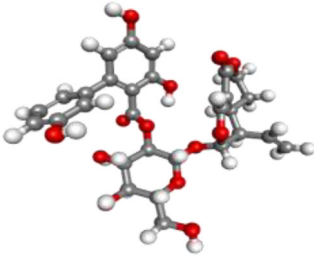
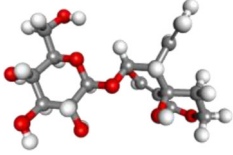
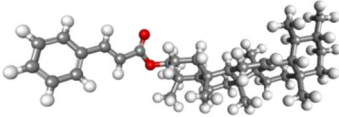
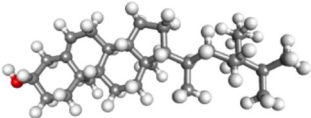
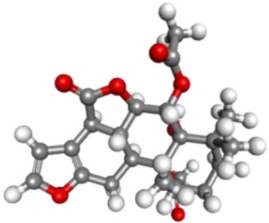
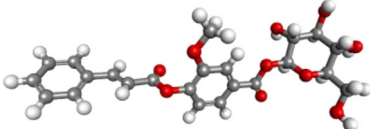
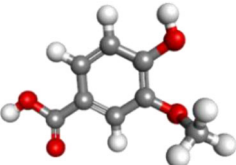
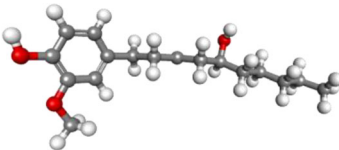
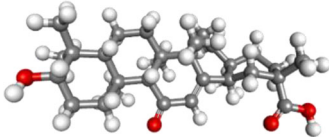
Studies of molecular targets are critical in discovering the phenotypic side effects or possible cross reactivity caused by the action of pharmaceutical agents. The mapping of bioactive small molecules is an essential method for deciphering the molecular pathways that are behind their bioactivity along with detection of potential adverse effects or cross-reactivity. Swiss Target Prediction website (<http://www.swisstargetprediction.ch>) was used for the target prediction of selected active constituents (Gfeller et al., 2014).

Results

Active constituents inhibits the activity of spike glycoprotein

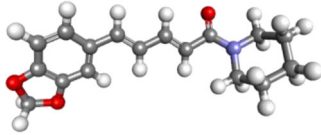
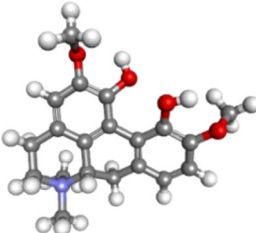
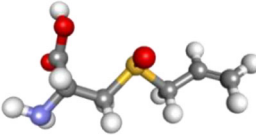
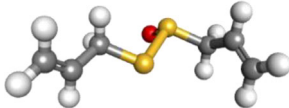
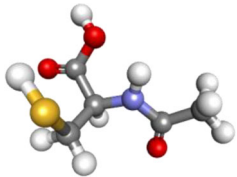
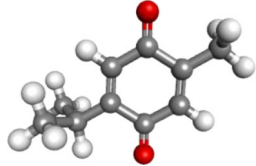
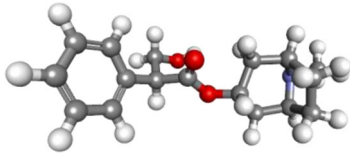
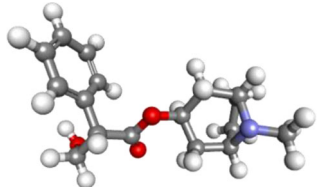
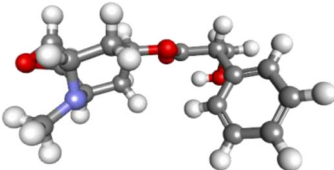
From 13 medicinal plants, we have identified 22 active constituents for this study based on the properties such as antiviral, antimicrobial, antiinflammatory and immunomodulatory activities. The binding energies of selected active constituents with spike glycoprotein and ACE2 were investigated and findings were reported in terms of the MolDock Ranking, interaction energy, H-bond energy and interaction of amino acid residues present at the active site of protein (Table 2). We have identified that 16 drugs exhibit strong affinity toward spike glycoprotein where 7 drugs have shown higher binding affinity than nafamostat (inhibitor of coronavirus spike glycoprotein). Nafamostat binds to spike glycoprotein and generate high MolDock Score (-114.633 kcal/mole), forms 5 hydrogen bonds with amino acid residues namely Ile312, Gln314, Ser316, and Arg765. We have found that amarogentin exhibits the highest binding affinity towards spike glycoprotein of SARS-CoV-2 followed by eufolatorin, α -amyrin, caesalpinins, kutkin, β -sitosterol, and belladonnine (Figure 1). Amarogentin binds to spike glycoprotein with 9 hydrogen bonds with amino acid residues namely Gln314, Ser735, Val736, Cys738, Thr739, Arg765, and Thr768 and generated a high MolDock score (-149.76 kcal/mole). In addition, drugs that also shown significant binding affinity toward spike glycoprotein are eufolatorin (MolDock score -140.6 kcal/mole and forms 3 hydrogen bonds with Lys304,

Table 1. Name of active constituents evaluated for in silico antiviral activity against SARS-CoV-2.

S. No	Name of active constituents	3D Structures	Pharmacological functions
	Amarogentin		Antitumorigenic, antidiabetic, antioxidant
	Sawertiamarine		Antioxidant, hepatoprotective, antidiabetic
	α -amyrin		Antiinflammatory, antifungal Antihyperglycemic
	β -sitosterol		Antiinflammatory, anticancer Antihyperglycemic
	Caesalpinins		Antioxidant, antibacterial, antiviral, antimalarial, antitumour, anticancer, antidiabetic, anthelmintic, antiinflammatory, analgesic, antipyretic, antiulcer, hepatoprotective, insecticidal
	Kutkin		Antiinflammatory, treatment of hepatitis
	Vanillic acid		Antioxidant, antiinflammatory, Chemo-preventive agent
	6-gingerol		Antiinflammatory, antioxidant, anticancer
	glycyrrhetic acid		Antiulcer, antiinflammatory, antiviral, hepatoprotective, antioxidant

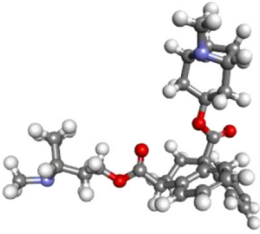
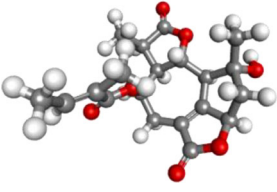
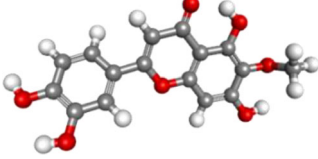
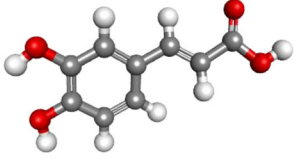
(continued)

Table 1. Continued.

S. No	Name of active constituents	3D Structures	Pharmacological functions
	Piperine		Antioxidant, antibacterial, antiviral, antimalarial, antitumour, anticancer, antidiabetic, antiinflammatory,
	Magnoflorine		Antidiabetic, antiinflammatory, neuropsychopharmacological, immunomodulatory, antioxidant, antifungal
	alliin		Treatment of atherosclerosis, diabetes, high blood pressure, high cholesterol level
	Allicin		Treatment of heart diseases, cancer
	N-acetylcysteine		Antioxidant, acetaminophen toxicity
	Thymoquinone		Antioxidant, antiinflammatory, anticancer
	Atropine		Pre-anesthetic agent, antispasmodic, Atropine is an antidote for organophosphate opium and chloroform poisoning.
	Hyoscyamine		Hyoscyamine is used for symptomatic relief in various gastrointestinal disorders such as peptic ulcers, spasms, and irritable bowel syndrome
	Scopolamine		Antidepressant, anxiolytic and treatment of motion sickness Scopolamine is stomach or intestinal problems, muscle spasms, and Parkinson-like conditions

(continued)

Table 1. Continued.

S. No	Name of active constituents	3D Structures	Pharmacological functions
	Belladonnine		Muscle relaxant, antispasmodic agent
	Eufoliatorin		Treatment of skin diseases
	Eupafolin		Treatment of skin diseases, antiinflammatory, anticancer
	Caffeic acid		Antioxidant, antimicrobial, antidiabetic, antiinflammatory, anticancer, neurodegenerative diseases, like Parkinson's disease.

Gln314, and Thr768), α -amyrin (MolDock score -137.72 kcal/mole and forms a hydrogen bond with Lys304), caesalpinins (MolDock score -132.45 kcal/mole and forms 5 hydrogen bonds with Lys304, Gln314, Asn764, and Arg765), kutkin (MolDock score -125.141 kcal/mole and forms 3 hydrogen bonds with Arg765, Thr768 and Gln957), β -sitosterol (MolDock score -119.68 kcal/mole and forms a hydrogen bond with Asn501), and belladonnine (MolDock score -117.0 kcal/mole and forms 4 hydrogen bonds with Gln314, Thr739 and Asn764). Besides these active constituents, molecules such as 6-gingerol, glycyrrhetic acid, piperine, sawertiamarine, magnoflorine, scopolamine, atropine, eupafolin, and hyoscyamine also have strong binding affinity towards spike glycoprotein and may be developed potential candidates against SARS-CoV-2 infection (supplementary Figures 1 and 2).

Active constituents inhibits the activity of angiotensin-converting enzyme 2

ACE2 is essential for entry of SARS-CoV-2 into the host cells. Therefore, targeting ACE2 may become a promising approach to design a potential attachment inhibitor for SARS-CoV-2. Our docking results revealed that amarogentin binds with high binding affinity with ACE2 as compared to captopril and other selected active constituents. Captopril binds to ACE2 with a binding score (MolDock Score of -73.69 kcal/mole and interaction energy -81.15 kcal/mole) and forms 3 hydrogen bonds with Glu402 and Asn394. Our

docking results suggested that apart from allicin, N-acetylcysteine, thymoquinone, vanillic acid, all the selected active constituents showed better binding affinity toward ACE2 protein compared to captopril. Amarogentin have highest interaction with ACE2 (MolDock Score -155.90 kcal/mole and 6 hydrogen bond with Asp350, Asp382, Tyr385, and Asn394) followed by kutkin (MolDock Score -138.70 kcal/mole and 3 hydrogen bonds with Asp350, Asp382), α -amyrin (MolDock Score -137.10 kcal/mole), belladonnine (MolDock Score -125.21 kcal/mole and 2 hydrogen bonds with Tyr385, Asn394), eupoliatrin ((MolDock Score -120.2 kcal/mole and 3 hydrogen bonds with Tyr385, Asn394 and His401), glycyrrhetic acid (MolDock Score -113.11 kcal/mole and 5 hydrogen bonds with Gln102, Asp382, Tyr385, and Lys562), piperine (MolDock Score -112.83 kcal/mole), caesalpinins (MolDock Score -112.28 kcal/mole and 3 hydrogen bonds with Asn394, Arg514, and Tyr515), 6-gingerol (MolDock Score -112.0 kcal/mole and 3 hydrogen bonds with Asp382, Glu398, and His401) (Figure 2). Other active constituents such as β -sitosterol, sawertiamarine, eupafolin, magnoflorine, scopolamine, atropine, hyoscyamine, caffeic acid and alliin also have considerable binding affinity toward ACE2 (supplementary Figures 3 and 4).

ADME analysis

The drug-likeness parameters of selected active constituents using swissADME are presented in (Table 3). An orally active pharmaceutical agent should not have molecular weight >

Table 2. Molecular docking results are indicated with maximum binding affinity of selected active constituents against SARS-CoV-2 spike glycoprotein and ACE2 along with MolDock Score and other parameters.

Source (Common/ Ayurveda or Sanskrit Name)	Active constituents	MolDock Score (KJ/mol)	Interaction (KJ/mol)	H-Bond (KJ/mol)	Interacting amino acid residues
Spike glycoprotein of SARS-CoV-2 (6VXX)					
<i>Swertia chirata</i> (<i>Chiretta/ Kiratatikta</i>)	Nafamostat	-114.63	-124.91	-8.55	Ile312, Gln314, Ser316, Thr761, Arg765
	Amarogentin	-149.76	-152.68	-10.28	Leu303, Gln314, Thr315, Ser735, Val736, Cys738, Thr739, Thr761, Arg765, Thr768
<i>Alstonia scholaris</i> (<i>Blackboard tree/ Saptacchada</i>)	Sawertiamarine	-94.60	-127.46	-24.25	Gln314, Ser316, Asn317, Arg765, Thr768
	α -amyrin	-137.72	-151.80	-2.16	Cys291, Cys301, Lys304, Tyr313, Gln314, Arg765
<i>Caesalpinia crista</i> (<i>Crested fever nut/ Kantaki karanja</i>)	β -sitosterol	-119.68	-127.22	0	Asn501
	Caesalpinins	-132.45	-141.75	-12.75	Lys304, Gln314, Asn764, Arg765
<i>Picrorhiza kurroa</i> (<i>Picrorhiza/ Kutki</i>)	Kutkin	-125.141	-142.90	-7.29	Arg765, Thr768, Gln951
	Vanillic acid	-63.70	-71.66	-8.01	Gln314, Asn764, Arg765, Thr768
<i>Zingiber officinale</i> (<i>Ginger/Singabera</i>)	6-gingerol	-107.57	-114.73	-2.61	Gln314, Ser316, Asp737, Arg765
	Glycyrrhetic acid	-106.04	-118.29	-9.26	Leu303, Ile312, Tyr313, Asn764, Arg765,
<i>Piper nigrum</i> (<i>Black Pepper/ Shyama</i>)	Piperine	-104.5	-110.91	-8.55	Gln314, Ser316, Asp737, Arg765, Thr768
	Magnoflorine	-93.15	-123.90	-10.19	Gln314, Thr31, Asn317, Asn764, Arg765, Thr768
<i>Tinospora cordifolia</i> (<i>Giloy/ Guduchi</i>)	Alliin	-63.56	-66.52	-8.97	Thr315, Asn764
	Allicin	-61.25	-58.35	-2.5	Gln314, Thr768
<i>Allium cepa</i> (<i>Onion/ Palandu</i>)	N-acetylcysteine	-63.13	-62.91	-17.38	Arg765, Gln957, Thr961, Lys964
	Thymoquinone	-61.58	-68.60	-2.18	Asn764, Arg765, Thr768
<i>Nigella sativa</i> (<i>Black Cumin/ Kalonji</i>)	Atropine	-88.45	-103.59	-5.68	Gln314, Thr315, Arg765, Thr768
	Hyoscyamine	-84.75	-96.93	-4.62	Thr302, Asn764, Arg765
<i>Atropa belladonna</i> (<i>Deadly nightshade/ Suchi</i>)	Scopolamine	-89.69	-110.58	-7.35	Gln314, Asn317, Asp737, Asn764, Arg765, Thr768
	Belladonnine	-117.0	-148.22	-10	Thr302, Gln314, Asn317, Thr739, Ser750, Thr761, Asn764, Arg765
<i>Artemisia vulgaris</i> (<i>Mugwort/ Nagadamani</i>)	Eufoliatorin	-140.6	-125.65	-6.46	Leu303, Lys304, Thr313, Gln314, Arg765, Thr768
	Eupafolin	-87.83	-117.53	-17.79	Thr302, Lys304, Arg765, Thr961, Lys964, Ser967, Ser968
Angiotensin-converting enzyme 2 (1R42)	Caffeic acid	-75.46	-82.88	-9.19	Gln314, Ser316, Asn317, Asn764
	Captopril	-73.69	-81.15	-13.07	His378, Asn394, Glu398, His401, Glu402
<i>Swertia chirata</i> (<i>Chiretta/ Kiratatikta</i>)	Amarogentin	-155.90	-146.99	-22.93	Thr347, Ala348, Trp349, Asp350, Asp382, Tyr385, Asn394
	Sawertiamarine	-101.27	-132.89	-15.91	Thr347, Ala348, Trp349, Asp350, Leu351, Asp382, Tyr385, Arg393, Phe400
<i>Alstonia scholaris</i> (<i>Blackboard tree/ Saptacchada</i>)	α -amyrin	-137.10	-154.63	0	Thr347, Ala348, His378, Phe390, Arg393, Phe400, His401
	β -sitosterol	-101.80	-122.70	-2.80	Glu375, His378, His401, Glu402, Cys562
<i>Caesalpinia crista</i> (<i>Crested fever nut/ Kantaki karanja</i>)	Caesalpinins	-112.28	-122.53	-5.38	His378, Asn394, Gly399, His401, Arg514, Tyr515, Arg518
	Kutkin	-138.70	-161.69	-16.26	Pro346, Ala348, Asp350, Glu375, His378, Asp382, His401
<i>Picrorhiza kurroa</i> (<i>Picrorhiza/ Kutki</i>)	Vanillic acid	-71.58	-81.02	-9.32	Asp206, Asn394, Gly395, His401
	6-gingerol	-112.0	-122.85	-12.61	Asp382, Glu398, His401, Lys562
<i>Zingiber officinale</i> (<i>Ginger/Singabera</i>)	6-gingerol	-112.0	-122.85	-12.61	Asp382, Glu398, His401, Lys562
	Glycyrrhetic acid	-113.11	-125.08	-13.50	Ala99, Gln102, Asp382, Tyr385, Phe390, Leu391, Arg393, Phe400, Lys562
<i>Piper nigrum</i> (<i>Black Pepper/ Shyama</i>)	Piperine	-112.83	-120.05	-1.10	Gly399, His401, Glu402, Arg514, Arg518
	Magnoflorine	-93.48	-122.75	-6.96	His378, Asn394, Asn397, His401, Glu402, Arg514
<i>Tinospora cordifolia</i> (<i>Giloy/ Guduchi</i>)	alliin	-76.30	-78.27	-11.94	Asn394, Asn397, Glu398, Phe400, His401, Arg514, Lys562
	Allicin	-59.90	-58.17	-2.48	Ala348, Tyr385, His378, Arg393, Phe400

(continued)

Table 2. Continued.

Source (Common/ Ayurveda or Sanskrit Name)	Active constituents	MolDock Score (KJ/mol)	Interaction (KJ/mol)	H-Bond (KJ/mol)	Interacting amino acid residues
<i>Allium cepa</i> (Onion/ Palandu)	N-acetylcysteine	-67.02	-69.64	-11.52	Asp350, Tyr385, Arg393
<i>Nigella sativa</i> (Black Cumin/ Kalonji)	Thymoquinone	-66.16	-73.29	-1.178	Asn394, Asn397, His401
<i>Atropa belladonna</i> (Deadly nightshade/ Suchi)	Atropine	-88.92	-108.57	-6.18	Trp349, Asp350, Asp382, His401, Ser440
	Hyoscyamine	-88.38	-103.03	-3.38	Ala348, Asp350, Tyr385, Arg393, Phe400
	Scopolamine	-89.25	-111.51	-5.00	Ala348, Tyr385, His401
	Belladonnine	-125.21	-162.17	-3.91	Ala348, His378, Tyr385, Phe390, Arg393, Asn394, Phe400, His401
<i>Artemisia vulgaris</i> (Mugwort/ Nagadamani)	Eufolatorin	-120.2	-106.46	-9.47	His378, Tyr385, Asn394, His401
	Eupafolin	-95.87	-121.14	-24.39	Pro346, Ala348, Glu375, His378, Asp382, Tyr385, Arg393, Asn394, His401, Zn804
	Caffeic acid	-79.04	-86.24	-11.52	Asn394, Gly395, Phe400, His401, Glu402, Arg514

*MolDock score: calculated by summing the external ligand interaction (protein–ligand interaction) and internal ligand interaction score. Interaction energy: The total energy between the pose and the protein (kJ/mol). H Bond energy: Hydrogen bonding energy (kJ/mol). Interacting residues: amino acid present on binding site and involved in various interactions with ligand.

500 g/mol, LogP > 5, hydrogen-bond-donating atoms > 5, hydrogen-bond-accepting atoms > 10, and topological polar surface > 140. The drug-likeness analysis suggested that all the active constituents follow the lipinski rule of five except amarogentin, α -amyrin, β -sitosterol, kutkin, glycyrrhetic acid and belladonnine. Further, ADME analysis revealed that most active constituents have high gastrointestinal absorption. Drugs such as amarogentin, sawertiamarine, α -amyrin and β -sitosterol have low gastro-intestinal absorption. The BBB permeability of active constituents was measured and it has been found that among the selected active constituents only 6-gingerol, piperine, magnoflorine, thymoquinone, atropine, hyoscyamine and belladonnine can cross the BBB (Figure 3). Cytochrome P450 (CYP) and P-glycoprotein (P-gp) protect tissues and organisms from foreign molecules. One can estimate that 50 to 90% of therapeutic molecules are substrates of five major isoforms (CYP1A2, CYP2C19, CYP2C9, CYP2D6, and CYP3A4). Inhibition of these iso-enzymes is certainly one major cause of pharmacokinetics related drug-drug interactions that results in accumulation, lower clearance of the drug or its metabolites leading to toxic or unwanted adverse effects of drugs. Therefore, the inhibitory activity of selected active constituents against these iso-enzymes were also measured and it is found that most of active constituents do not interfere with the activity of CYP1A2, CYP2D6, CYP2C9, CYP2C19, and CYP3A4 (Table 4).

Toxicity analysis

Predicting toxicology of small molecules is necessary to predict the amount of tolerability of the small molecule before being ingested into models of humans and animals. Our toxicity analysis suggested that none of the active constituents were associated with hepatotoxicity and cytotoxicity. Active constituents like α -amyrin, glycyrrhetic acid, piperine, eufolatorin eupafolin and caffeic acid may associate with carcinogenicity. In the same way, amarogentin, α -amyrin, β -sitosterol, caesalpinins, kutkin, 6-gingerol, glycyrrhetic acid, piperine, magnoflorine, eufolatorin and eupafolin may have immunotoxicity; N-acetylcysteine may associate with

mutagenicity. Further, the probable toxicities of active constituents with various Tox21 nuclear receptor signalling pathways and Tox21-stress response pathways were calculated and presented in Table 5.

Gene network and pathway analysis

Gene network analysis was performed to predict a set of genes and associated pathways that may be significantly altered during COVID-19. The literature search revealed that *TMPRSS2*, *ACE2*, *IL2*, *IL2RB*, *IL6*, *IL7*, *CXCL8*, *IL10*, *CSF3*, *CXCL10*, *CCL2*, *CCL3*, *TNF*, *IL1B*, *TGFB1*, *CTSL*, *CTSB*, *DDIT4*, *RRAS*, *CTSD*, *BIRC5*, *TNFSF10*, *CTS2*, *NTRK1*, *IGFBP3*, *TP53I3*, *CCNB1*, *RRM2*, *CCNB2*, *GTSE1*, *CDK1*, *STEAP3*, *CXCL1*, *CXCL2*, *CCL3*, *CCL4*, and *CXCL6* were found to be differentially expressed during COVID-19 (Kong et al., 2020; Li, Chen, et al., 2020; Li, Li, et al., 2020; Qi et al., 2020; Wang & Xu, 2020; Xiong et al., 2020; Xu et al., 2020). A genome-wide map of human genetic interactions was inferred from the gene network analysis which revealed the involvement of crucial signaling pathways including G-protein coupled receptor binding (*CCL2*, *CCL3*, *CCL4*, *CXCL3*, *CXCL8*, *CXCL9*, *CXCL10*, and *CXCL11*); regulation of intracellular transport (*TNF*, *TGFB1*, *NFKB1A*, *IL1B*, *IL6*, *IL10*, *CSF3*); protein kinase B signaling (*TNF*, *TGFB1*, *CCL2*, *CCL3*, *IL1B*, *CSF3*); protein import into nucleus (*TNF*, *TGFB1*, *NFKB1A*, *IL1B*, *IL6*, *IL10*, *CSF3*); protein secretion (*STEAP3*, *TNF*, *TGFB1*, *IL6*, *IL10*, *CCL3*, *CSF3*); peptidyl-serine phosphorylation (*DDIT4*, *CDK1*, *TNF*, *TGFB1*, *NFKB1A*, *IL1B*, *IL6*, *IL10*, *CSF3*, *CXCL9*, *CXCL10*); nuclear transport (*TNF*, *TGFB1*, *IL1B*, *IL6*, *IL10*, *CSF3*); extrinsic apoptotic signaling pathway (*TNF*, *TGFB1*, *IL1B*, *TNFAIP3*, *TNFSF10*); cellular response to tumor necrosis factor (*TNF*, *CCL2*, *CCL3*, *CXCL8*); response to virus (*ACE2*, *TNF*, *TNFAIP3*, *IL6*, *CCL4*); regulation of angiotensin levels in blood (*ACE2*, *CTS2*); regulation of JAK-STAT cascade (*IL2*, *IL6*, *IL20*); positive regulation of ion transport (*CCL3*, *CCL4*, *IL1B*, *CXCL9*, *CXCL10*) and membrane protein proteolysis (*TNF*, *IL1B*, *IL10*) (Figure 4). Based on this information, we found some common pathways involved in the pathogenesis of COVID-19 which were also targeted by the selected active constituents during target prediction analysis.

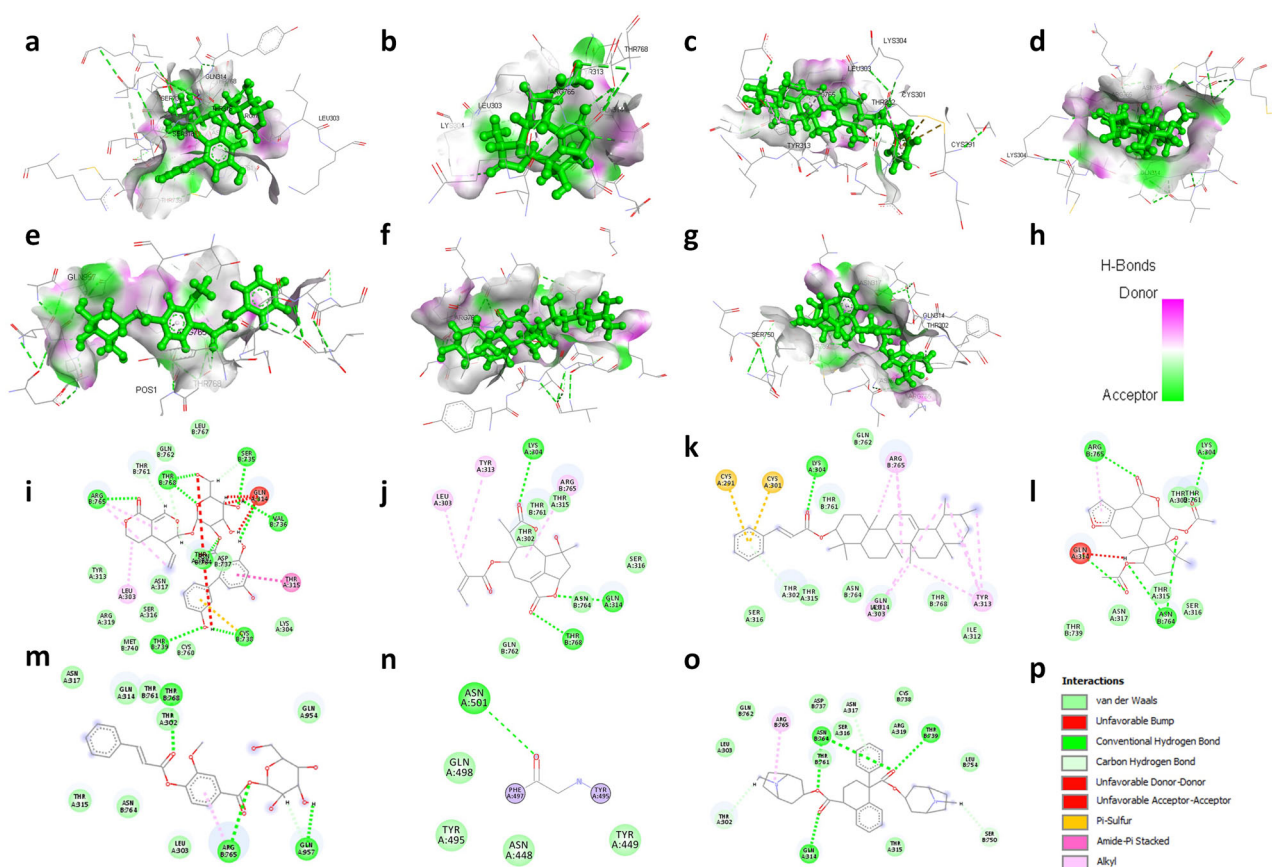


Figure 1. 3D structural views of ligand-binding site. The 3D structures display H-bond interactions (green dashed lines) of ligands (a) amarogentin (b) eufoliatorin, (c) α -amyrin, (d) caesalpinins, (e) kutkin, (f) β -sitosterol, and (g) belladonnine and (h) represent the color intensity of hydrogen bonds with the Spike glycoprotein of SARS-CoV-2 (6VXX). The i, j, k, l, m, n, o demonstrated the 2D structural views of ligand-binding site of amarogentin, eufoliatorin, α -amyrin, caesalpinins, kutkin, β -sitosterol, belladonnine and p represents the H-bonding (dark green circles associated with the green dashed lines); van der Waals forces (medium light green circles); carbon-oxygen dipole-dipole interaction (light green circles with dashed lines); alkyl-pi interactions (light pink circles with dashed lines); T-shaped pi-pi stacking and (parallel) pi-pi stacking (both indicated with dark violet circles); cation-pi interaction (orange circle). The blue halo surrounding the interacting residues represents the solvent accessible surface that is proportional to its diameter. Images were generated using Discovery Studio Visualizer 4.5.

Target prediction analysis

Drug–target interactions (DTIs) is a newer approach that provides accurate prediction of interactions formed between a drug and its targeted protein via computational approaches and helps in the discovery of novel targets for natural products. The target prediction analysis revealed that the selected active constituents can act on a number of targets such as family A G-protein coupled receptor, protease, electrochemical transporter, oxidoreductase, hydrolase, enzyme, nuclear receptor, phosphatase, cytochrome P-450, taste family of G-protein coupled receptor membrane protein, secreted protein, ligand-gated ion channel, kinase, transferase, membrane receptors, ligase, family C G-protein coupled receptor, transcription factors, primary active transporter, and phosphodiesterase and regulate the factions of these targets (Figure 5). Further, target accuracy of active constituents was compared with the proposed inhibitors of spike glycoprotein and ACE2 (nafamostat and captopril) and some common targets like protease, electrochemical transporter, family A G-protein coupled receptor, ligand-gated ion channel, hydrolase, enzyme, and membrane receptors have identified between active constituents and proposed inhibitors (supplementary Figure 5). This makes an inference that the selected active constituents may act on the similar pathways as directed by proposed inhibitors.

Discussion

SARS-CoV-2 is the etiological agent responsible for the COVID-19 outbreak (Dai et al., 2020). The disease rapidly spread to more than 200 countries and was declared as a global health emergency by the WHO. There are currently no clinically effective vaccines or specific antiviral medicines for the prevention and treatment of COVID-19. Although various drugs and vaccines are tested in clinical trials, the effectiveness of these drugs or vaccines is still not confirmed in humans. Drugs such as hydroxychloroquine, traditional Chinese medicines (TCM), methylprednisolone, human immunoglobulin, interferons, chloroquine, arbidol, oseltamivir, remdesivir, favipiravir, ritonavir, bevacizumab, lopinavir, combination therapy of hydroxychloroquine and azithromycin have been tested against SARS-CoV-2 infection (Maurya et al., 2020; Rosa & Santos, 2020). Patients treated with chloroquine or hydroxychloroquine in combination with azithromycin have developed serious heart rhythm complications (prolongation of QT interval and ventricular tachycardia). Food and Drug Administration (FDA) has not approved the use chloroquine and hydroxychloroquine for the treatment COVID-19 (www.fda.gov/drugs/drug-safety-and-availability/fda-cautions-against-use-hydroxychloroquine-or-chloroquine-covid-19-outside-hospital-setting-or).

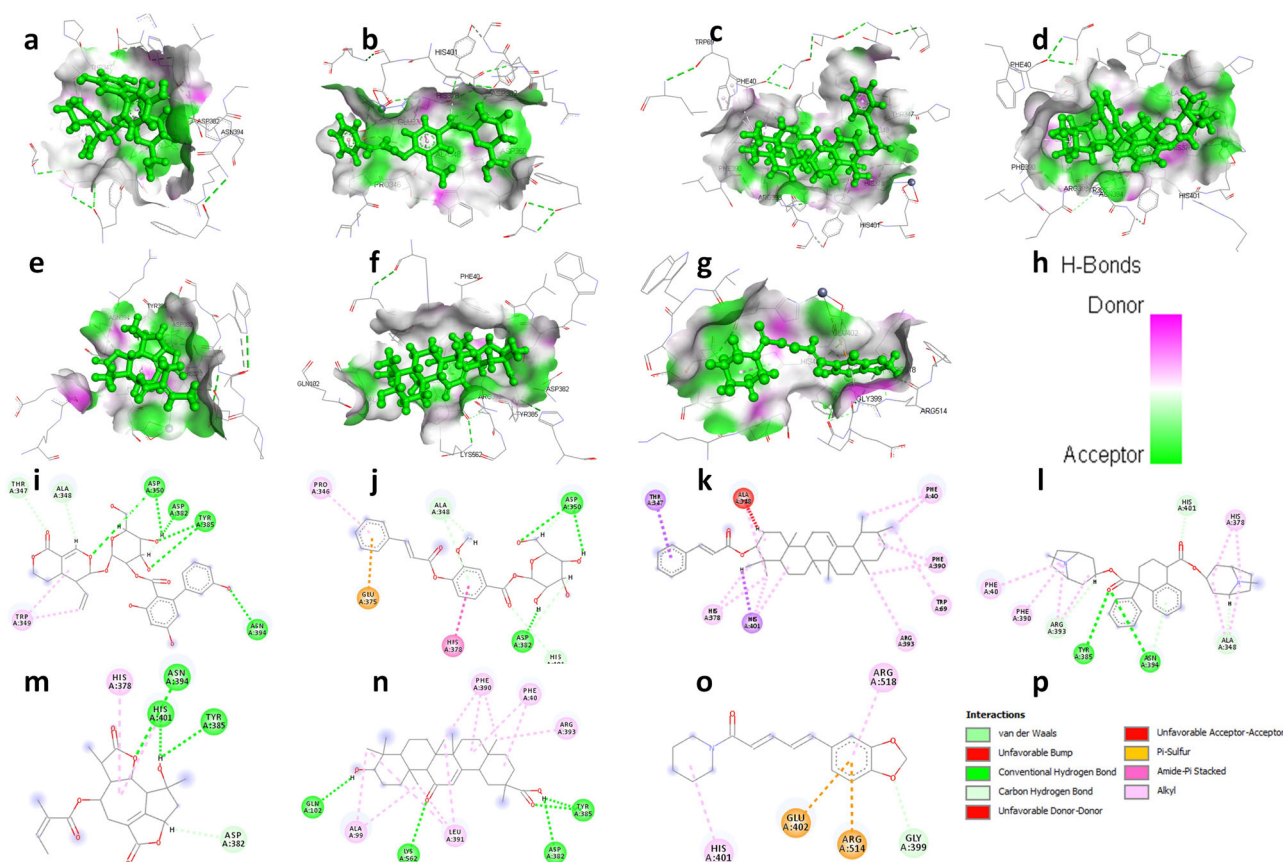


Figure 2. 3D structural views of ligand-binding site. The 3D structures display H-bond interactions (green dashed lines) of ligands (a) amarogentin (b) kutkin, (c) α -amyryn, (d) belladonnine, (e) eufoliatorin, (f) glycyrrhetic acid, (g) piperine and (h) represent the color intensity of hydrogen bonds with the Angiotensin-converting enzyme-2 (1R42). The i, j, k, l, m, n, o demonstrated the 2D structural views of ligand-binding site of amarogentin, kutkin, α -amyryn, belladonnine, eufoliatorin, glycyrrhetic acid, piperine and p represents the H-bonding (dark green circles associated with the green dashed lines); van der Waals forces (medium light green circles); carbon-oxygen dipole-dipole interaction (light green circles with dashed lines); alkyl-pi interactions (light pink circles with dashed lines); T-shaped pi-pi stacking and (parallel) pi-pi stacking (both indicated with dark violet circles); cation-pi interaction (orange circle). The blue halo surrounding the interacting residues represents the solvent accessible surface that is proportional to its diameter. Images were generated using Discovery Studio Visualizer 4.5.

Plants are a perfect source for identifying potential and cost-effective medicinal drugs during humanitarian emergencies. The repurposing of these natural products may accelerate the drug discovery process during virus outbreaks (Newman & Cragg, 2020). The selected natural plants which are used in this study reported having a number of pharmacological activities. Plants such as *Alstonia scholaris*, *Picrorhiza kurroa*, *Swertia chirata*, and *Caesalpinia crista* were primarily known for their anti-malarial anti-inflammatory, anti-allergic, hepatoprotective activities (Baliga, 2012; Kumar & Van Staden, 2015; Ravi et al., 2018; Verma et al., 2009). *Zingiber officinale*, *Glycyrrhiza glabra*, *Pippur nigrum*, *Tinospora cordifolia*, *Allium sativum*, and *Allium cepa*, is primarily known for analgesic antimicrobial, immunomodulatory and antioxidants properties. *Nigella sativa* is also known for antidiabetic, anti-cancer, immunomodulatory, antimicrobial, anti-inflammatory, spasmolytic, bronchodilator (Hosseini et al., 2014; Pandey et al., 2013). *Atropa belladonna* and *Artemisia vulgaris* are used as analgesic, muscle relaxants, hypolipidemic, anti-inflammatory, immunostimulating agent, antiplasmodial properties, and management of neurological disorders (El-Tantawy, 2015; Owais et al., 2014).

The active constituents present in selected plants were evaluated for the prediction of potential attachment

inhibitors against SARS-CoV-2 via targeting spike glycoprotein as well as its host receptor ACE2. Docking results demonstrate that active constituents like amarogentin, eufoliatorin, α -amyryn, caesalpinins, kutkin, β -sitosterol, and belladonnine have stronger affinity toward spike glycoprotein than nafamostat. Similarly, amarogentin, kutkin, α -amyryn, belladonnine, eufoliatorin, glycyrrhetic acid, piperine, caesalpinins, and 6-gingerol have been screened as top molecules that demonstrated higher binding affinity toward ACE2 compared with captopril. Thus, this result provides an opportunity for development of potential attachment inhibitor among amarogentin eufoliatorin, α -amyryn, caesalpinins, kutkin, β -sitosterol, and belladonnine in the absence of specific therapy for COVID-19.

The physicochemical and pharmacokinetic properties are important for the pharmacological activity of drugs (Lipinski, 2004). Most of the active constituents have properties of druggability with good oral bioavailability. In addition, active constituents such as amarogentin, α -amyryn, β -sitosterol, kutkin, glycyrrhetic acid and belladonnine may have less oral bioavailability. However, various methods are available to improve oral drug absorption, including preparation of pro-drugs and drug conjugates, improving the drug solubility and dissolution rate, use of permeation enhancers and co-

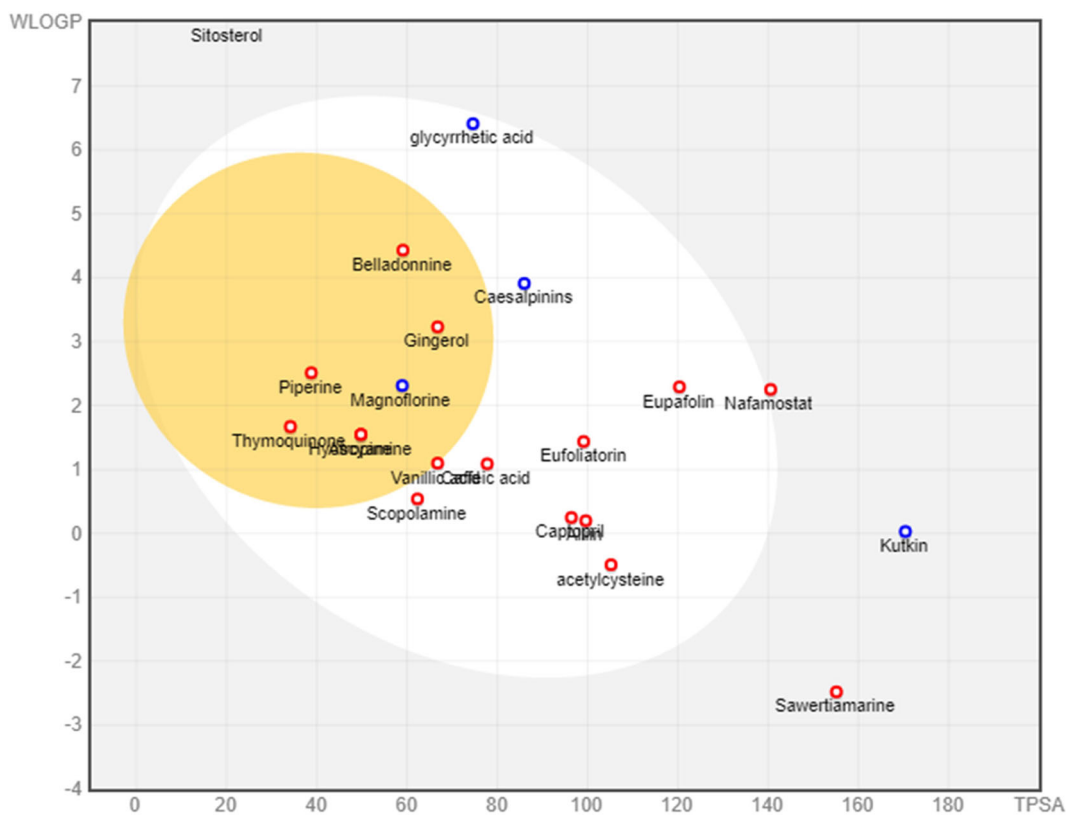


Figure 3. Biodistribution and absorption analysis. The biodistribution and absorption profiles of active constituents and control drugs are shown using the half boiled eggs model. Points located in BOILED-Eggs yolk are molecules predicted to passively permeate through the blood-brain barrier. Points located in the BOILED-Eggs white are molecules predicted to be passively absorbed by the gastrointestinal tract. Blue dots are for molecules predicted to be effluated from the central nervous system by the P-glycoprotein. Red dots are for molecules not to be effluated from the central nervous system by the P-glycoprotein.

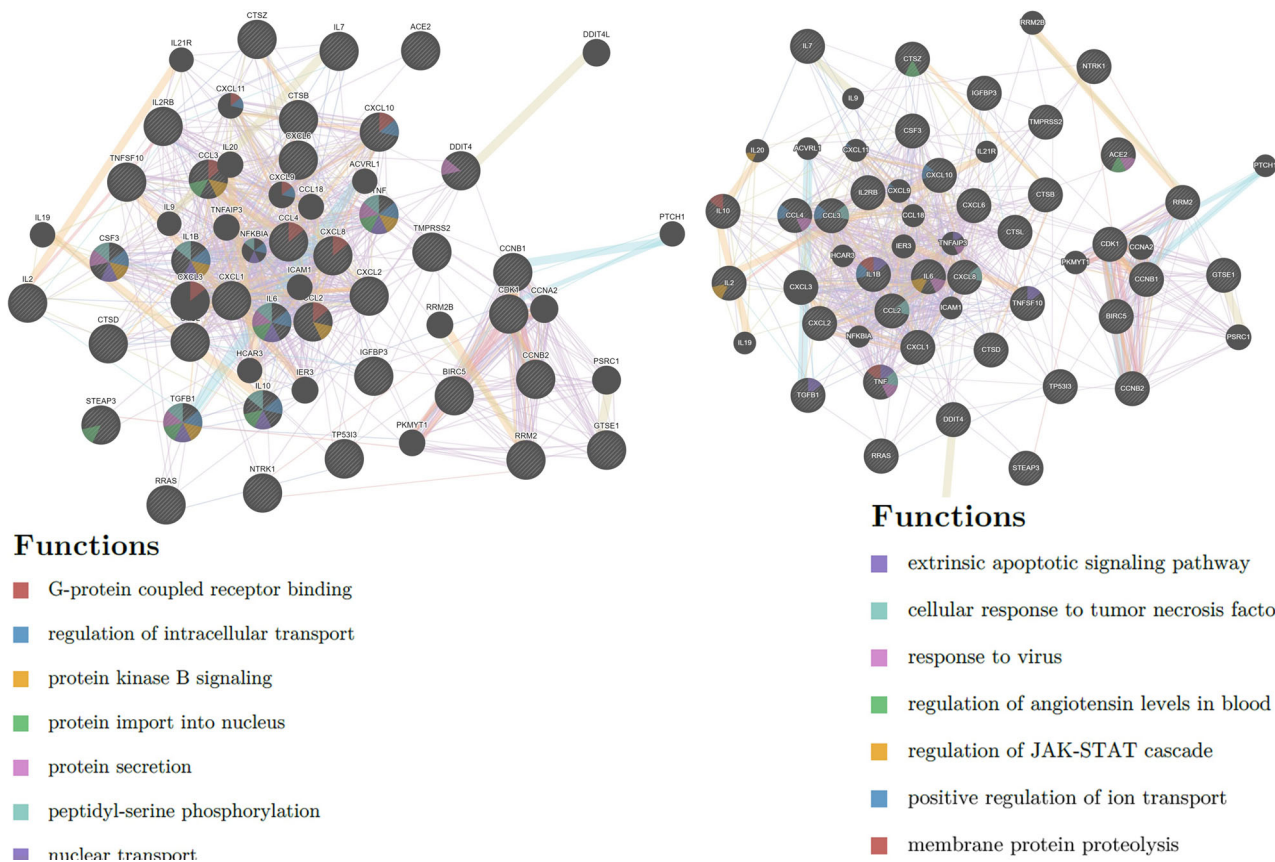


Figure 4. Gene network analysis demonstrated set of genes and associated pathways that may be significantly altered during COVID-19 analyzed using GeneMANIA web server.

Table 3. Drug likeness properties of selected active constituents.

Ligand	Molecular formula	Molecular Weight (g/mol)	LogP	Hydrogen Bond Donor	Hydrogen Bond Acceptor	Topological Polar Surface Area (Å ²)	Lipinski #violations
Amarogentin	C ₂₉ H ₃₀ O ₁₃	586.54	2.46	6	13	201.67	3
Sawertiamarine	C ₁₆ H ₂₂ O ₁₀	374.34	1.74	5	10	155.14	0
α-amyrin	C ₃₂ H ₅₂ O ₂	468.75	5.19	0	2	26.3	1
β-sitosterol	C ₂₉ H ₅₀ O	414.71	4.79	1	1	20.23	1
Caesalpinins	C ₂₄ H ₃₂ O ₆	416.51	3.06	1	6	85.97	0
Kutkin	C ₂₃ H ₂₈ O ₁₂	496.46	2.09	6	12	170.44	2
Vanillic acid	C ₈ H ₈ O ₄	168.15	1.4	2	4	66.76	0
6-gingerol	C ₁₇ H ₂₆ O ₄	294.39	3.48	2	4	66.76	0
Glycyrrhetic acid	C ₃₀ H ₄₆ O ₄	470.68	3.56	2	4	74.6	1
Piperine	C ₁₇ H ₁₉ NO ₃	285.34	3.42	0	3	38.77	0
Magnoflorine	C ₂₀ H ₂₄ NO ₄	342.41	-0.59	2	4	58.92	0
Alliin	C ₆ H ₁₁ NO ₃ S	177.22	0.55	2	4	99.6	0
acetylcysteine	C ₅ H ₉ NO ₃ S	163.19	0.65	2	3	105.2	0
Thymoquinone	C ₁₀ H ₁₂ O ₂	164.2	1.99	0	2	34.14	0
Atropine	C ₁₇ H ₂₃ NO ₃	289.37	2.85	1	4	49.77	0
Hyoscyamine	C ₁₇ H ₂₃ NO ₃	289.37	2.85	1	4	49.77	0
Scopolamine	C ₁₇ H ₂₁ NO ₄	303.35	2.74	1	5	62.3	0
Belladonnine	C ₃₄ H ₄₂ N ₂ O ₄	542.71	4.95	0	6	59.08	2
Eufoliorin	C ₂₀ H ₂₄ O ₇	376.4	2.37	1	7	99.13	0
Eupafolin	C ₁₆ H ₁₂ O ₇	316.26	2.13	4	7	120.36	0
Caffeic acid	C ₉ H ₈ O ₄	180.16	0.97	3	4	77.76	0

Table 4. Pharmacokinetics properties of selected active constituents analyzed by swissADME server.

Name	GIA	BBB	P-gp substrate	CYP1A2 inhibitor	CYP2C19 inhibitor	CYP2C9 inhibitor	CYP2D6 inhibitor	CYP3A4 inhibitor
Amarogentin	Low	No	Yes	No	No	No	No	No
Sawertiamarine	Low	No	No	No	No	No	No	No
α-amyrin	Low	No	No	No	No	No	No	No
β-sitosterol	Low	No	No	No	No	No	No	No
Caesalpinins	High	No	Yes	No	No	No	Yes	Yes
Kutkin	Low	No	Yes	No	No	No	No	No
Vanillic acid	High	No	No	No	No	No	No	No
6-gingerol	High	Yes	No	Yes	No	No	Yes	No
Glycyrrhetic acid	High	No	Yes	No	No	No	No	No
Piperine	High	Yes	No	Yes	Yes	Yes	No	No
Magnoflorine	High	Yes	Yes	Yes	No	No	No	Yes
Alliin	High	No	No	No	No	No	No	No
acetylcysteine	High	No	No	No	No	No	No	No
Thymoquinone	High	Yes	No	No	No	No	No	No
Atropine	High	Yes	No	No	No	No	Yes	No
Hyoscyamine	High	Yes	No	No	No	No	Yes	No
Scopolamine	High	No	No	No	No	No	Yes	No
Belladonnine	High	Yes	No	No	No	Yes	No	Yes
Eufoliorin	High	No	No	No	No	No	No	No
Eupafolin	High	No	No	Yes	No	No	Yes	Yes
Caffeic acid	High	No	No	No	No	No	No	No

administration with delivery agents (Zhao et al., 2019). Besides these methods, various nanotechnology based approaches like liposomes, solid lipid nanoparticles, polymeric nanoparticles, magnetic nanoparticles, and nanoemulsion are available that increases the oral absorption, BBB permeability, and facilitates the targeted delivery of natural products with reduced toxicity (Vaiserman et al., 2019). In order to determine the safety and efficacy of drugs in the biological system, the information of pharmacokinetics and the toxicity profile of drugs are important. The ADME data of active constituents demonstrated good gastrointestinal absorption, BBB permeability and are predicted as either non-substrates or non-inhibitors of *CYP1A2*, *CYP3A4*, *CYP2D6*, *CYP2C9*, and *CYP2C19*, enzymes. The ability of active constituents to cross the BBB can be used for the effective management of neurological complications arising during COVID-19. Finally, these active constituents are allowed for toxicity prediction and interestingly, most of the active constituents are

inactive for hepatotoxicity, carcinogenicity, immunotoxicity, mutagenicity, cytotoxicity, Tox21 nuclear receptor signalling pathways, and Tox21-stress response pathways.

At last, target prediction and gene network was performed to identify crucial pathways involved in pathogenesis of COVID-19 and the pathways targeted by the active constituents. The gene network analysis suggests that involvement of G-protein coupled receptor, regulation of intracellular transport, protein kinase B signaling, protein secretion, peptidyl-serine phosphorylation, nuclear transport, extrinsic apoptotic signaling pathway, cellular response to tumor necrosis factor, regulation of angiotensin levels in blood, positive regulation of ion transport, and membrane protein proteolysis in the pathogenesis of COVID-19. These pathways are known to perform crucial functions like neurotransmission, regulation of sense of vision, regulation of blood pressure, smell, taste, and pain, regulation of transport of bio-chemicals, glucose metabolism, cell proliferation,

Table 5. Toxicity parameters of selected active constituents analyzed by ProTox-II server.

Parameters	Amaroge-ntin	Sawerti-amarine	α -Amyrin	β -Sitosterol	Caesalpinins	Kutkin
<i>Organ Toxicity</i>						
Hepatotoxicity	Inactive	Inactive	Inactive	Inactive	Inactive	Inactive
<i>Toxicity end points</i>						
Carcinogenicity	Inactive	Inactive	Active	Inactive	Inactive	Inactive
Immunotoxicity	Active	Inactive	Active	Active	Active	Active
Mutagenicity	Inactive	Inactive	Inactive	Inactive	Inactive	Inactive
Cytotoxicity	Inactive	Inactive	Inactive	Inactive	Inactive	Inactive
<i>Tox21 Nuclear receptor signalling pathways</i>						
AhR	Inactive	Inactive	Inactive	Inactive	Inactive	Inactive
AR	Inactive	Inactive	Active	Inactive	Inactive	Inactive
AR-LBD	Inactive	Inactive	Active	Inactive	Inactive	Inactive
Aromatase	Inactive	Inactive	Inactive	Inactive	Inactive	Inactive
ER	Inactive	Inactive	Inactive	Inactive	Inactive	Inactive
ER-LBD	Inactive	Inactive	Inactive	Inactive	Inactive	Inactive
PPAR-Gamma	Inactive	Inactive	Inactive	Inactive	Inactive	Inactive
<i>Tox21 Stress response pathways</i>						
nrf2/ARE	Inactive	Inactive	Inactive	Inactive	Inactive	Inactive
HSE	Inactive	Inactive	Inactive	Inactive	Inactive	Inactive
MMP	Inactive	Inactive	Inactive	Inactive	Inactive	Inactive
Phosphoprotein (Tumor Suppressor) p53	Inactive	Inactive	Inactive	Inactive	Inactive	Inactive
ATAD5	Inactive	Inactive	Inactive	Inactive	Inactive	Inactive
LD ₅₀ (mg/kg)	2000	2000	4800	890	244	2260
Prediction accuracy	67.8%	100%	70.97%	72.9%	54.26%	68.07%
Parameters	Vanillic acid	6-Gingerol	Glycyrrhetic acid	Piperine	Magnoflorine	Alliin
<i>Organ Toxicity</i>						
Hepatotoxicity	Inactive	Inactive	Inactive	Inactive	Inactive	Inactive
<i>Toxicity end points</i>						
Carcinogenicity	Inactive	Inactive	Active	Active	Inactive	Inactive
Immunotoxicity	Inactive	Active	Active	Active	Active	Inactive
Mutagenicity	Inactive	Inactive	Inactive	Inactive	Inactive	Inactive
Cytotoxicity	Inactive	Inactive	Inactive	Inactive	Inactive	Inactive
<i>Tox21 Nuclear receptor signalling pathways</i>						
AhR	Inactive	Inactive	Inactive	Active	Inactive	Inactive
AR	Inactive	Inactive	Inactive	Inactive	Inactive	Inactive
AR-LBD	Inactive	Inactive	Inactive	Inactive	Inactive	Inactive
Aromatase	Inactive	Inactive	Inactive	Inactive	Inactive	Inactive
ER	Inactive	Inactive	Inactive	Active	Inactive	Inactive
ER-LBD	Inactive	Inactive	Inactive	Inactive	Inactive	Inactive
PPAR-Gamma	Inactive	Inactive	Inactive	Inactive	Inactive	Inactive
<i>Tox21 Stress response pathways</i>						
nrf2/ARE	Inactive	Inactive	Active	Inactive	Inactive	Inactive
HSE	Inactive	Inactive	Active	Inactive	Inactive	Inactive
MMP	Inactive	Inactive	Inactive	Inactive	Inactive	Inactive
Phosphoprotein (Tumor Suppressor) p53	Inactive	Inactive	Inactive	Inactive	Inactive	Inactive
ATAD5	Inactive	Inactive	Inactive	Active	Inactive	Inactive
LD ₅₀ (mg/kg)	2000	250	560	330	350	8000
Prediction accuracy	69.26%	100%	100%	100%	72.9%	68.07%
Parameters	Allicin	N-Acetylcys-teine	Thymoquin-one	Atropine	Hyoscyamine	Scopolam-ine
<i>Organ Toxicity</i>						
Hepatotoxicity	Inactive	Inactive	Inactive	Inactive	Inactive	Inactive
<i>Toxicity end points</i>						
Carcinogenicity	Inactive	Inactive	Inactive	Inactive	Inactive	Inactive
Immunotoxicity	Inactive	Inactive	Inactive	Inactive	Inactive	Inactive
Mutagenicity	Inactive	Active	Inactive	Inactive	Inactive	Inactive
Cytotoxicity	Inactive	Inactive	Inactive	Inactive	Inactive	Inactive
<i>Tox21 Nuclear receptor signalling pathways</i>						
AhR	Inactive	Inactive	Inactive	Inactive	Inactive	Inactive
AR	Inactive	Inactive	Inactive	Inactive	Inactive	Inactive
AR-LBD	Inactive	Inactive	Inactive	Inactive	Inactive	Inactive
Aromatase	Inactive	Inactive	Inactive	Inactive	Inactive	Inactive
ER	Inactive	Inactive	Inactive	Inactive	Inactive	Active
ER-LBD	Inactive	Inactive	Inactive	Inactive	Inactive	Inactive
PPAR-Gamma	Inactive	Inactive	Inactive	Inactive	Inactive	Inactive
<i>Tox21 Stress response pathways</i>						
nrf2/ARE	Inactive	Inactive	Inactive	Inactive	Inactive	Inactive
HSE	Inactive	Inactive	Inactive	Inactive	Inactive	Inactive
MMP	Inactive	Inactive	Active	Inactive	Inactive	Inactive
Phosphoprotein (TumorSupressor) p53	Inactive	Inactive	Inactive	Inactive	Inactive	Inactive
ATAD5	Inactive	Inactive	Inactive	Inactive	Inactive	Inactive
LD ₅₀ (mg/kg)	874	4400	2400	75	75	270
Prediction accuracy	54.26%	100%	100%	100%	100%	100%

(continued)

Table 5. Continued.

Parameters	Amaroge-ntin	Sawerti-amarine	α -Amyrin	β -Sitosterol	Caesalpinins	Kutkin
Parameters	Belladon-nine	Eufoliato-rin	Eupafolin	Caffeic acid	Nafamostat	Captopril
<i>Organ Toxicity</i>						
Hepatotoxicity	Inactive	Inactive	Inactive	Inactive	Active	Inactive
Toxicity end points						
Carcinogenicity	Inactive	Active	Active	Active	Active	Active
Immunotoxicity	Inactive	Active	Active	Inactive	Inactive	Inactive
Mutagenicity	Inactive	Inactive	Inactive	Inactive	Active	Inactive
Cytotoxicity	Inactive	Inactive	Inactive	Inactive	Inactive	Inactive
<i>Tox21 Nuclear receptor signalling pathways</i>						
AhR	Inactive	Inactive	Active	Inactive	Active	Inactive
AR	Inactive	Inactive	Inactive	Active	Inactive	Inactive
AR-LBD	Inactive	Inactive	Inactive	Inactive	Inactive	Inactive
Aromatase	Inactive	Inactive	Inactive	Inactive	Inactive	Inactive
ER	Inactive	Inactive	Active	Inactive	Inactive	Inactive
ER-LBD	Inactive	Inactive	Active	Inactive	Inactive	Inactive
PPAR-Gamma	Inactive	Inactive	Inactive	Inactive	Inactive	Inactive
<i>Tox21 Stress response pathways</i>						
nrf2/ARE	Inactive	Inactive	Inactive	Inactive	Inactive	Inactive
HSE	Inactive	Inactive	Inactive	Inactive	Inactive	Inactive
MMP	Inactive	Inactive	Active	Inactive	Inactive	Inactive
Phosphoprotein (Tumor Suppressor) p53	Inactive	Inactive	Inactive	Inactive	Inactive	Inactive
ATAD5	Inactive	Inactive	Inactive	Inactive	Inactive	Inactive
LD ₅₀ (mg/kg)	570	1330	3919	2980	3050	2078
Prediction accuracy	100%	69.26%	70.97%	70.97%	68.07%	100%

Aryl hydrocarbon Receptor (AhR), Androgen Receptor (AR), Androgen Receptor Ligand Binding Domain (AR-LBD), Aromatase, Estrogen Receptor Alpha (ER), Estrogen Receptor Ligand Binding Domain (ER-LBD), Peroxisome Proliferator Activated Receptor Gamma (PPAR-Gamma), Nuclear factor (erythroid-derived 2)-like 2/antioxidant responsive element (nrf2/ARE), Heat shock factor response element (HSE), Mitochondrial Membrane Potential (MMP), Phosphoprotein (Tumor Suppressor) p53, ATPase family AAA domain-containing protein 5 (ATAD5).

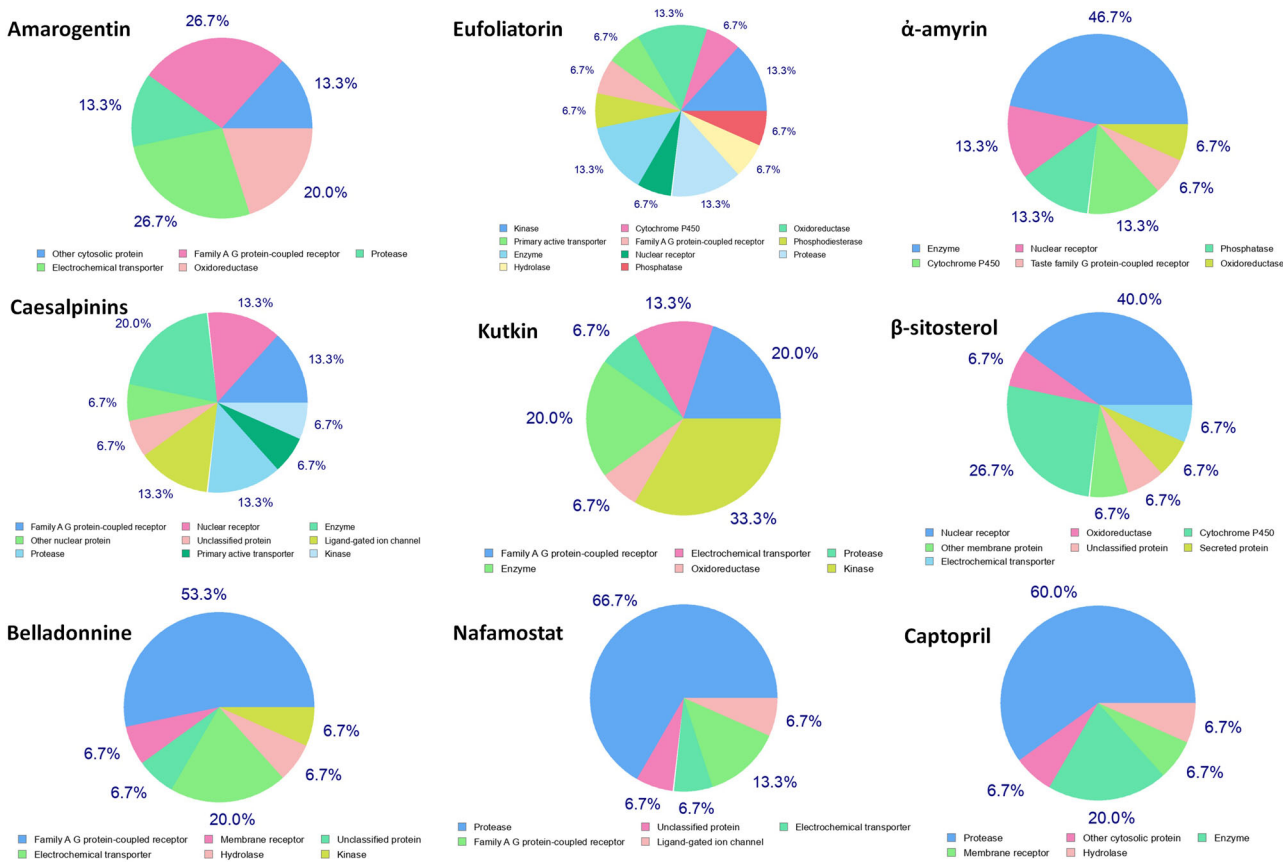


Figure 5. Major targets are listed for active constituent and control drugs identified using target prediction analysis. Some common targets like protease, electrochemical transporter, family A G-protein coupled receptor, ligand-gated ion channel, hydrolase, enzyme, and membrane receptors have been identified between active constituents and control drugs.

transcription, apoptosis, and cell migration adhesion, adaptation, cell survival, and receptor for pharmaceutical agents. Dysfunctioning of these pathways may affect the normal

homeostasis and associated with conditions weakening of immune system, inflammation, auto-immune diseases, cancer and involved in various pathological events caused due to

the virus infections (Keating & Striker, 2012; Londino et al., 2017; Mages et al., 2008; Meineke et al., 2019; Naderer & Fulcher, 2018; Paludan & Mogensen, 2001; Ye, 2013; Zhang et al., 2016). The patients infected with SARS-CoV-2 can develop symptoms like neurological complications (Guillain-Barre syndrome, encephalopathy, hemorrhagic encephalopathy, dizziness, myalgia anosmia, encephalitis, necrotising stroke, epileptic seizures, and rhabdomyolysis), loss of taste, increased cellular apoptosis, and high level of chemokines, and cytokines (Carod-Artal, 2020; Chen et al., 2020; Guzzi et al., 2020; Mehta et al., 2020; Zheng et al., 2020). Therefore, targeting these pathways may help in the better management of COVID-19. Our drug–target interactions analysis suggests that most of the active constituents can act on these pathways and regulate their functions and this may help to establish active constituents as an evidence-based therapy for the management of COVID-19.

Conclusions

Based on the findings of this study, it is confirmed that investigated active constituents can interfere with the important amino acids to inhibit the activity of spike glycoprotein of SARS-CoV-2 as well as ACE2. The results suggested that amarogentin, eufoliorin, α -amyrin, caesalpinins, kutkin, β -sitosterol, and belladonnine are the top ranked molecules have the highest affinity towards both the spike glycoprotein and ACE2. Further, drug-likeness, pharmacokinetics, and toxicity parameters of the active constituents were calculated and it is found that most of the active constituents have passed the criteria of drug-like molecule and demonstrated good pharmacokinetic profile with minimum predicted toxicity level. gene network analysis confirmed that G-protein coupled receptor, regulation of intracellular transport, protein kinase B signaling, protein secretion, peptidyl-serine phosphorylation, nuclear transport, extrinsic apoptotic signaling pathway, cellular response to tumor necrosis factor, regulation of angiotensin levels in blood, positive regulation of ion transport, and membrane protein proteolysis were altered during COVID-19. At last, target prediction study demonstrated that most active constituents can effectively target the pathways which are altered during COVID-19. Therefore, the anticipated outcomes of this study will allow us to understand the probable antiviral role of the selected active constituents against SARS-CoV-2 infection and established as potential evidence-based therapy for patients diagnosed with COVID-19 in the absence of specific therapy.

Acknowledgements

The authors are grateful to the Vice Chancellor, King George's Medical University (KGMU), Lucknow, India for the encouragement for this work. The authors have no other relevant affiliations or financial involvement with any organization or entity with a financial interest in or financial conflict with the subject matter or materials discussed in the manuscript apart from those disclosed.

Disclosure statement

The authors declare no conflict of interest.

ORCID

Shailendra K. Saxena  <https://orcid.org/0000-0003-2856-4185>

References

- Andersen, K. G., Rambaut, A., Lipkin, W. I., Holmes, E. C., & Garry, R. F. (2020). The proximal origin of SARS-CoV-2. *Nature Medicine*, 26(4), 450–452. <https://doi.org/10.1038/s41591-020-0820-9>
- Baliga, M. S. (2012). Review of the phytochemical, pharmacological and toxicological properties of *Alstonia Scholaris* Linn. R. Br (Saptaparna). *Chinese Journal of Integrative Medicine, Advance Online Publication*. <https://doi.org/10.1007/s11655-011-0947-0>
- Banerjee, P., Eckert, A. O., Schrey, A. K., & Preissner, R. (2018). ProTox-II: A webserver for the prediction of toxicity of chemicals. *Nucleic Acids Research*, 46(W1), W257–W263. <https://doi.org/10.1093/nar/gky318>
- Belouzard, S., Millet, J. K., Licitra, B. N., & Whittaker, G. R. (2012). Mechanisms of coronavirus cell entry mediated by the viral spike protein. *Viruses*, 4(6), 1011–1033. <https://doi.org/10.3390/v4061011>
- Carod-Artal, F. J. (2020). Neurological complications of coronavirus and COVID-19. *Complicaciones neurológicas por coronavirus y COVID-19. Revista de Neurología*, 70(9), 311–322. <https://doi.org/10.33588/rn.7009.2020179>
- Chen, X., Zhao, B., Qu, Y., Chen, Y., Xiong, J., Feng, Y., Men, D., Huang, Q., Liu, Y., Yang, B., Ding, J., & Li, F. (2020). Detectable serum SARS-CoV-2 viral load (RNAemia) is closely correlated with drastically elevated interleukin 6 (IL-6) levels in critically ill COVID-19 patients. *Clinical Infectious Diseases*, <https://doi.org/10.1093/cid/ciaa449>
- Chen, N., Zhou, M., Dong, X., Qu, J., Gong, F., Han, Y., Qiu, Y., Wang, J., Liu, Y., Wei, Y., Xia, J., Yu, T., Zhang, X., & Zhang, L. (2020). Epidemiological and clinical characteristics of 99 cases of 2019 novel coronavirus pneumonia in Wuhan, China: A descriptive study. *The Lancet*, 395(10223), 507–513. England, [https://doi.org/10.1016/S0140-6736\(20\)30211-7](https://doi.org/10.1016/S0140-6736(20)30211-7)
- Dai, W., Zhang, B., Jiang, X.-M., Su, H., Li, J., Zhao, Y., Xie, X., Jin, Z., Peng, J., Liu, F., Li, C., Li, Y., Bai, F., Wang, H., Cheng, X., Cen, X., Hu, S., Yang, X., Wang, J., ... Liu, H. (2020). Structure-based design of antiviral drug candidates targeting the SARS-CoV-2 main protease. *Science (New York, N.Y.)*, 368(6497), 1331–1335. <https://doi.org/10.1126/science.abb4489>
- Daina, A., Michielin, O., & Zoete, V. (2017). SwissADME: A free web tool to evaluate pharmacokinetics, drug-likeness and medicinal chemistry friendliness of small molecules. *Scientific Reports*, 7, 42717. <https://doi.org/10.1038/srep42717>
- El-Tantawy, W. H. (2015). Biochemical effects, hypolipidemic and anti-inflammatory activities of *Artemisia vulgaris* extract in hypercholesterolemic rats. *Journal of Clinical Biochemistry and Nutrition*, 57(1), 33–38. <https://doi.org/10.3164/jcfn.14-141>
- Food and drug administration. FDA cautions against use of hydroxychloroquine or chloroquine for COVID-19 outside of the hospital setting or a clinical trial due to risk of heart rhythm problems. <https://www.fda.gov/drugs/drug-safety-and-availability/fda-cautions-against-use-hydroxychloroquine-or-chloroquine-covid-19-outside-hospital-setting-or>.
- Franz, M., Rodriguez, H., Lopes, C., Zuberi, K., Montojo, J., Bader, G. D., & Morris, Q. (2018). GeneMANIA update 2018. *Nucleic Acids Research*, 46(W1), W60–W64. <https://doi.org/10.1093/nar/gky311>
- Gfeller, D., Grosdidier, A., Wirth, M., Daina, A., Michielin, O., & Zoete, V. (2014). SwissTargetPrediction: A web server for target prediction of bioactive small molecules. *Nucleic Acids Research*, 42(Web Server issue), W32–W38. <https://doi.org/10.1093/nar/gku293>
- Guan, W.-J., Ni, Z.-Y., Hu, Y., Liang, W.-H., Ou, C.-Q., He, J.-X., Liu, L., Shan, H., Lei, C.-L., Hui, D. S. C., Du, B., Li, L.-J., Zeng, G., Yuen, K.-Y., Chen, R.-C., Tang, C.-L., Wang, T., Chen, P.-Y., Xiang, J., ... Zhong, N.-S. (2020). China medical treatment expert group for Covid-19 (2020). Clinical characteristics of coronavirus disease 2019 in China. *The New England Journal of Medicine*, 382(18), 1708–1720. <https://doi.org/10.1056/NEJMoa2002032>

- Guo, Y. R., Cao, Q. D., Hong, Z. S., Tan, Y. Y., Chen, S. D., Jin, H. J., Tan, K. S., Wang, D. Y., & Yan, Y. (2020). The origin, transmission and clinical therapies on coronavirus disease 2019 (COVID-19) outbreak - an update on the status. *Military Medical Research*, 7(1), 11. <https://doi.org/10.1186/s40779-020-00240-0>
- Guzzi, P. H., Mercatelli, D., Ceraolo, C., & Giorgi, F. M. (2020). Master regulator analysis of the SARS-CoV-2/human interactome. *Journal of Clinical Medicine*, 9(4), 982. <https://doi.org/10.3390/jcm9040982>
- Hosseini, A., Shafiee-Nick, R., & Mousavi, S. H. (2014). Combination of *Nigella sativa* with *Glycyrrhiza glabra* and *Zingiber officinale* augments their protective effects on doxorubicin-induced toxicity in h9c2 cells. *Iranian Journal of Basic Medical Sciences*, 17(12), 993–1000.
- Keating, J. A., & Striker, R. (2012). Phosphorylation events during viral infections provide potential therapeutic targets. *Reviews in Medical Virology*, 22(3), 166–181. <https://doi.org/10.1002/rmv.722>
- Kong, Q., Xiang, Z., Wu, Y., Gu, Y., Guo, J., & Geng, F. (2020). Analysis of the susceptibility of lung cancer patients to SARS-CoV-2 infection. *Molecular Cancer*, 19(1), 80. <https://doi.org/10.1186/s12943-020-01209-2>
- Kumar, S., Maurya, V. K., Prasad, A. K., Bhatt, M., & Saxena, S. K. (2020). Structural, glycosylation and antigenic variation between 2019 novel coronavirus (2019-nCoV) and SARS coronavirus (SARS-CoV). *VirusDisease*, 31(1), 13–21. <https://doi.org/10.1007/s13337-020-00571-5>
- Kumar, S., Nyodu, R., Maurya, V. K., & Saxena, S. K. (2020). Morphology, Genome Organization, Replication, and Pathogenesis of Severe Acute Respiratory Syndrome Coronavirus 2 (SARS-CoV-2). In *Coronavirus Disease 2019 (COVID-19)* (pp. 23–31). Springer. https://doi.org/10.1007/978-981-15-4814-7_3
- Kumar, V., & Van Staden, J. (2015). A Review of *Swertia chirayita* (Gentianaceae) as a Traditional Medicinal Plant. *Frontiers in Pharmacology*, 6, 308. <https://doi.org/10.3389/fphar.2015.00308>
- Li, M., Chen, L., Zhang, J., Xiong, C., & Li, X. (2020). The SARS-CoV-2 receptor ACE2 expression of maternal-fetal interface and fetal organs by single-cell transcriptome study. *PLoS One*, 15(4), e0230295. <https://doi.org/10.1371/journal.pone.0230295>
- Li, G., & De Clercq, E. (2020). Therapeutic options for the 2019 novel coronavirus (2019-nCoV). *Nature reviews. Drug Discovery*, 19(3), 149–150. <https://doi.org/10.1038/d41573-020-00016-0>
- Li, M. Y., Li, L., Zhang, Y., & Wang, X. S. (2020). Expression of the SARS-CoV-2 cell receptor gene ACE2 in a wide variety of human tissues. *Infectious Diseases of Poverty*, 9(1), 45. <https://doi.org/10.1186/s40249-020-00662-x>
- Lipinski, C. A. (2004). Lead- and drug-like compounds: The rule-of-five revolution. *Drug Discovery Today. Technologies*, 1(4), 337–341. <https://doi.org/10.1016/j.ddtec.2004.11.007>
- Londino, J. D., Lazrak, A., Collawn, J. F., Bebok, Z., Harrod, K. S., & Matalon, S. (2017). Influenza virus infection alters ion channel function of airway and alveolar cells: Mechanisms and physiological sequelae. *American Journal of Physiology. Lung Cellular and Molecular Physiology*, 313(5), L845–L858. <https://doi.org/10.1152/ajplung.00244.2017>
- Mages, J., Freimüller, K., Lang, R., Hatzopoulos, A. K., Guggemoos, S., Koszinowski, U. H., & Adler, H. (2008). Proteins of the secretory pathway govern virus productivity during lytic gammaherpesvirus infection. *Journal of Cellular and Molecular Medicine*, 12(5B), 1974–1989. <https://doi.org/10.1111/j.1582-4934.2008.00235.x>
- Maurya, V. K., Kumar, S., Bhatt, M. L., & Saxena, S. K. (2020). Therapeutic Development and Drugs for the Treatment of COVID-19. In *Coronavirus Disease 2019 (COVID-19)*. (pp. 109–126). Springer. https://doi.org/10.1007/978-981-15-4814-7_10
- Maurya, V. K., Kumar, S., Prasad, A. K., Bhatt, M. L., & Saxena, S. K. (2020). Structure-based drug designing for potential antiviral activity of selected natural products from Ayurveda against SARS-CoV-2 spike glycoprotein and its cellular receptor. *VirusDisease*, 31(2), 179–193. <https://doi.org/10.1007/s13337-020-00598-8>
- Mehta, P., McAuley, D. F., Brown, M., Sanchez, E., Tattersall, R. S., & Manson, J. J. (2020). COVID-19: Consider cytokine storm syndromes and immunosuppression. *Lancet (London, England)*, 395(10229), 1033–1034. [https://doi.org/10.1016/S0140-6736\(20\)30628-0](https://doi.org/10.1016/S0140-6736(20)30628-0)
- Meineke, R., Rimmelzwaan, G. F., & Elbahesh, H. (2019). Influenza virus infections and cellular kinases. *Viruses*, 11(2), 171. <https://doi.org/10.3390/v11020171>
- Naderer, T., & Fulcher, M. C. (2018). Targeting apoptosis pathways in infections. *Journal of Leukocyte Biology*, 103(2), 275–285. <https://doi.org/10.1189/JLB.4MR0717-286R>
- Newman, D. J., & Cragg, G. M. (2020). Natural Products as Sources of New Drugs over the Nearly Four Decades from 01/1981 to 09/2019. *Journal of Natural Products*, 83(3), 770–803. <https://doi.org/10.1021/acs.jnatprod.9b01285>
- Owais, F., Anwar, S., Saeed, F., Muhammad, S., Ishtiaque, S., & Mohiuddin, O. (2014). Analgesic, Anti-inflammatory and neuropharmacological effects of *Atropa belladonna*. *Pakistan Journal of Pharmaceutical Sciences*, 27(6), 2183–2187.
- Paludan, S. R., & Mogensen, S. C. (2001). Virus-cell interactions regulating induction of tumor necrosis factor alpha production in macrophages infected with herpes simplex virus. *Journal of Virology*, 75(21), 10170–10178. <https://doi.org/10.1128/JVI.75.21.10170-10178.2001>
- Pandey, M. M., Rastogi, S., & Rawat, A. K. (2013). Indian traditional ayurvedic system of medicine and nutritional supplementation. *Evidence-Based Complementary and Alternative Medicine : Ecamp*, 2013, 376327. <https://doi.org/10.1155/2013/376327>
- Qi, F., Qian, S., Zhang, S., & Zhang, Z. (2020). Single cell RNA sequencing of 13 human tissues identify cell types and receptors of human coronaviruses. *Biochemical and Biophysical Research Communications*, 526(1), 135–140. <https://doi.org/10.1016/j.bbrc.2020.03.044>
- Ravi, S. K., Ramesh, B. N., Munduguru, R., & Vincent, B. (2018). Multiple pharmacological activities of *Caesalpinia crista* against aluminium-induced neurodegeneration in rats: Relevance for Alzheimer's disease. *Environmental Toxicology and Pharmacology*, 58, 202–211. <https://doi.org/10.1016/j.etap.2018.01.008>
- Rosa, S., & Santos, W. C. (2020). Clinical trials on drug repositioning for COVID-19 treatment. *Revista Panamericana de Salud Publica = Pan American Journal of Public Health*, 44, e40. e40. <https://doi.org/10.26633/RPSP.2020.40>
- Singhal, T. (2020). A Review of Coronavirus Disease-2019 (COVID-19). *Indian Journal of Pediatrics*, 87(4), 281–286. <https://doi.org/10.1007/s12098-020-03263-6>
- Thomsen, R., & Christensen, M. H. (2006). MolDock: A new technique for high-accuracy molecular docking. *Journal of Medicinal Chemistry*, 49(11), 3315–3321. <https://doi.org/10.1021/jm051197e>
- Towler, P., Staker, B., Prasad, S. G., Menon, S., Tang, J., Parsons, T., Ryan, D., Fisher, M., Williams, D., Dales, N. A., Patane, M. A., & Pantoliano, M. W. (2004). ACE2 X-ray structures reveal a large hinge-bending motion important for inhibitor binding and catalysis. *The Journal of Biological Chemistry*, 279(17), 17996–18007. <https://doi.org/10.1074/jbc.M311191200>
- Vaiserman, A., Koliada, A., Zayachkivska, A., & Lushchak, O. (2019). Nanodelivery of Natural Antioxidants: An Anti-aging Perspective. *Frontiers in Bioengineering and Biotechnology*, 7, 447. <https://doi.org/10.3389/fbioe.2019.00447>
- Verma, P. C., Basu, V., Gupta, V., Saxena, G., & Rahman, L. U. (2009). Pharmacology and chemistry of a potent hepatoprotective compound Picroliv isolated from the roots and rhizomes of *Picrorhiza kurroa* royle ex benth. (kutki). *Curr Pharm Biotechnol*, 10(6), 641–649. <https://doi.org/10.2174/138920109789069314>
- Walls, A. C., Park, Y. J., Tortorici, M. A., Wall, A., McGuire, A. T., & Velesler, D. (2020). Structure, function, and antigenicity of the SARS-CoV-2 Spike glycoprotein. *Cell*, 181(2), 281–292.e6. <https://doi.org/10.1016/j.cell.2020.02.058>
- Wang, Z., & Xu, X. (2020). scRNA-seq Profiling of human testes reveals the presence of the ACE2 receptor, A target for SARS-CoV-2 infection in Spermatogonia, Leydig and Sertoli Cells. *Cells*, 9(4), 920. E920. <https://doi.org/10.3390/cells9040920>
- World health organization. Coronavirus disease (COVID-19) Pandemic. <https://www.who.int/emergencies/diseases/novel-coronavirus-2019>
- Xiong, Y., Liu, Y., Cao, L., Wang, D., Guo, M., Jiang, A., Guo, D., Hu, W., Yang, J., Tang, Z., Wu, H., Lin, Y., Zhang, M., Zhang, Q., Shi, M., Liu, Y., Zhou, Y., Lan, K., & Chen, Y. (2020). Transcriptomic characteristics of bronchoalveolar lavage fluid and peripheral blood mononuclear cells in COVID-19 patients. *Emerging Microbes & Infections*, 9(1), 761–770. <https://doi.org/10.1080/22221751.2020.1747363>
- Xu, H., Zhong, L., Deng, J., Peng, J., Dan, H., Zeng, X., Li, T., & Chen, Q. (2020). High expression of ACE2 receptor of 2019-nCoV on the

- epithelial cells of oral mucosa. *International Journal of Oral Science*, 12(1), 8 <https://doi.org/10.1038/s41368-020-0074-x>
- Ye, J. (2013). Roles of regulated intramembrane proteolysis in virus infection and antiviral immunity. *Biochimica et Biophysica Acta*, 1828(12), 2926–2932. <https://doi.org/10.1016/j.bbamem.2013.05.005>
- Zhang, J., Feng, H., Xu, S., & Feng, P. (2016). Hijacking GPCRs by viral pathogens and tumor. *Biochemical Pharmacology*, 114, 69–81. <https://doi.org/10.1016/j.bcp.2016.03.021>
- Zhao, J., Yang, J., & Xie, Y. (2019). Improvement strategies for the oral bioavailability of poorly water-soluble flavonoids: An overview. *International Journal of Pharmaceutics*, 570, 118642 <https://doi.org/10.1016/j.ijpharm.2019.118642>
- Zheng, H. Y., Zhang, M., Yang, C. X., Zhang, N., Wang, X. C., Yang, X. P., Dong, X. Q., & Zheng, Y. T. (2020). Elevated exhaustion levels and reduced functional diversity of T cells in peripheral blood may predict severe progression in COVID-19 patients. *Cellular & Molecular Immunology*, 17(5), 541–543. <https://doi.org/10.1038/s41423-020-0401-3>